



Development of 3-methyl/3-(morpholinomethyl)benzofuran derivatives as novel antitumor agents towards non-small cell lung cancer cells

Mohammad M. Al-Sanea, Ghada H. Al-Ansary, Zainab M. Elsayed, Raed M. Maklad, Eslam B. Elkaeed, Mohamed A. Abdelgawad, Syed Nasir Abbas Bukhari, Marwa M. Abdel-Aziz, Howayda Suliman & Wagdy M. Eldehna

To cite this article: Mohammad M. Al-Sanea, Ghada H. Al-Ansary, Zainab M. Elsayed, Raed M. Maklad, Eslam B. Elkaeed, Mohamed A. Abdelgawad, Syed Nasir Abbas Bukhari, Marwa M. Abdel-Aziz, Howayda Suliman & Wagdy M. Eldehna (2021) Development of 3-methyl/3-(morpholinomethyl)benzofuran derivatives as novel antitumor agents towards non-small cell lung cancer cells, Journal of Enzyme Inhibition and Medicinal Chemistry, 36:1, 987-999, DOI: 10.1080/14756366.2021.1915302

To link to this article: <https://doi.org/10.1080/14756366.2021.1915302>



© 2021 The Author(s). Published by Informa UK Limited, trading as Taylor & Francis Group.



[View supplementary material](#)



Published online: 13 May 2021.



[Submit your article to this journal](#)



Article views: 634



[View related articles](#)



[View Crossmark data](#)



Citing articles: 1 [View citing articles](#)

RESEARCH PAPER



Development of 3-methyl/3-(morpholinomethyl)benzofuran derivatives as novel antitumor agents towards non-small cell lung cancer cells

Mohammad M. Al-Sanea^a, Ghada H. Al-Ansary^{b,c}, Zainab M. Elsayed^d, Raed M. Maklad^{e,f}, Eslam B. Elkaeed^{g,h}, Mohamed A. Abdelgawad^{a,i}, Syed Nasir Abbas Bukhari^a, Marwa M. Abdel-Aziz^j, Howayda Suliman^k and Wagdy M. Eldehna^e

^aDepartment of Pharmaceutical Chemistry, College of Pharmacy, Jouf University, Sakaka, Saudi Arabia; ^bDepartment of Pharmaceutical Chemistry, Pharmacy Program, Batterejee Medical College, Jeddah, Saudi Arabia; ^cDepartment of Pharmaceutical Chemistry, Faculty of Pharmacy, Ain Shams University, Cairo, Egypt; ^dScientific Research and Innovation Support Unit, Faculty of Pharmacy, Kafrelsheikh University, Kafrelsheikh, Egypt; ^eDepartment of Pharmaceutical Chemistry, Faculty of Pharmacy, Kafrelsheikh University, Kafrelsheikh, Egypt; ^fInstitute of Drug Discovery and Development, Kafrelsheikh University, Kafrelsheikh, Egypt; ^gDepartment of Pharmaceutical Sciences, College of Pharmacy, AlMaarefa University, Ad Diriyah, Riyadh, Saudi Arabia; ^hDepartment of Pharmaceutical Organic Chemistry, Faculty of Pharmacy (Boys), Al-Azhar University, Nasr City, Cairo, Egypt; ⁱDepartment of Pharmaceutical Organic Chemistry, Faculty of Pharmacy, Beni-Suef University, Beni-Suef, Egypt; ^jThe Regional Center for Mycology & Biotechnology, Al-Azhar University, Cairo, Egypt; ^kDepartment of Medical Biochemistry, Faculty of Medicine, Alexandria University, Alexandria, Egypt

ABSTRACT

As one of the most lethal malignancies, lung cancer is considered to account for approximately one-fifth of all malignant tumours-related deaths worldwide. This study reports the synthesis and *in vitro* biological assessment of two sets of 3-methylbenzofurans (**4a–d**, **6a–c**, **8a–c** and **11**) and 3-(morpholinomethyl)benzofurans (**15a–c**, **16a–b**, **17a–b** and **18**) as potential anticancer agents towards non-small cell lung carcinoma A549 and NCI-H23 cell lines, with VEGFR-2 inhibitory activity. The target benzofuran-based derivatives efficiently inhibited the growth of both A549 and NCI-H23 cell lines with IC₅₀ spanning in ranges 1.48–47.02 and 0.49–68.9 μM, respectively. The three most active benzofurans (**4b**, **15a** and **16a**) were further investigated for their effects on the cell cycle progression and apoptosis in A549 (for **4b**) and NCI-H23 (for **15a** and **16a**) cell lines. Furthermore, benzofurans **4b**, **15a** and **16a** displayed good VEGFR-2 inhibitory activity with IC₅₀ equal 77.97, 132.5 and 45.4 nM, respectively.

ARTICLE HISTORY

Received 28 February 2021
Revised 2 April 2021
Accepted 6 April 2021

KEYWORDS

Benzofuran-2-carbohydra-
zide; anticancer agents;
lung cancer; VEGFR-
2 inhibitors

1. Introduction







Worldwide, lung cancer ranks the most commonly diagnosed cancer as the number of cases reported for both sexes merged in 2018 exceeds 2 million new cases accounting for 11.6% of total cases and 1.8 million lung cancer deaths which presents 18.4% of the total cancer deaths globally^{1,2}. Although lung cancer is more commonly diagnosed in males due to the higher incidence of smoking, yet it is reported to be the second cause of death among females, preceded by breast cancer². Accordingly, for the last few decades, it has been the interest and concern of scientists to explore new molecules that exhibit significant antiproliferative activity against the invading lung cancer in the aim of combating such global health problem³. Interestingly, many of the discovered molecules proved clinical success for the management of lung cancer^{4–6}. Yet, the urgent need for more effective and selective novel anticancer agents is an inevitable necessity which provokes more rationalised scientific research.


Benzofurans are regarded as privileged scaffolds upon which many molecules are pursued that proved clinical utility in many fields of medical research^{7,8}. Benzofuran derivatives tagged with

diverse pharmacophoric groups proved to possess multiple pharmacological activities for the past decades^{9,10}. Among these pharmacological activities, benzofuran derivatives exhibit significant inhibitory carbonic anhydrase^{11,12}, antioxidant¹³, anti-Alzheimer's¹⁴, anti-inflammatory¹⁵, antibacterial^{15,16}, anti-tubercular¹⁷, as well as anticancer activities¹⁸. Benzofurans were reported to exert their antiproliferative activities through diverse mechanisms of cellular proliferation inhibition including apoptosis induction^{19–23} and VEGFR-2 inhibitory action^{24–26}.

The tumour growth mostly depends on the angiogenesis process that guarantees formation of new blood vessels from an existing vasculature²⁷. Angiogenesis process is mainly orchestrated by diverse pro-angiogenic and anti-angiogenic factors formed by the tumour cells as well as the host cells. Among the pro-angiogenic growth factors, vascular endothelial growth factors (VEGFs) and its receptor VEGFR-2 exert a significant impact on the angiogenesis process²⁷. Over the past decade, it was well-established that inhibition of VEGFR-2 is a favourable strategy to afford efficient anticancer agents²⁸.

Fruquintinib (Elunate[®], Figure 1) is a potent, selective and orally bioavailable benzofuran-based VEGFR-2 inhibitor²⁹.

CONTACT Wagdy M. Eldehna  wagdy2000@gmail.com  Department of Pharmaceutical Chemistry, Faculty of Pharmacy, Kafrelsheikh University, Kafrelsheikh 33516, Egypt; Mohammad M. Al-Sanea  mohmah80@gmail.com  Department of Pharmaceutical Chemistry, College of Pharmacy, Jouf University, Sakaka, Aljulf 72341, Saudi Arabia; Ghada H. Al-Ansary  ghada.yassin@bmc.edu.sa  Department of Pharmaceutical Chemistry, Pharmacy Program, Batterejee Medical College, Jeddah, Saudi Arabia

 Supplemental data for this article can be accessed [here](#).

© 2021 The Author(s). Published by Informa UK Limited, trading as Taylor & Francis Group.

This is an Open Access article distributed under the terms of the Creative Commons Attribution License (<http://creativecommons.org/licenses/by/4.0/>), which permits unrestricted use, distribution, and reproduction in any medium, provided the original work is properly cited.

Fruquintinib has received its first global approval in China, in 2018, for treatment of metastatic colorectal cancer³⁰. Currently, Fruquintinib is being evaluated in phase III clinical trials for

treatment of advanced gastric cancer and advanced NSCLC³¹. Furthermore, PF-00337210 (Figure 1), another benzofuran-based small molecule, is an orally bioavailable potent inhibitor of VEGFR-2 that is currently tested in the clinical trials³².

As a part of our ongoing tireless research for discovering novel anticancer molecules, we herein reported six novel series of benzofuran derivatives. Our design strategy proceeds as two sets of benzofuran series. The first set is the 3-methylbenzofurans; **4a-d**, **6a-c**, **8a-c** and **11** (Figure 1), whereas the second set is the benzofuran series tagged with morpholino group; 3-(morpholinomethyl)benzofurans: **15a-c**, **16a-b**, **17a-b** and **18** (Figure 1). All the synthesised benzofurans were evaluated for their antiproliferative activities against lung A549 and NCI-H23 cancer cell lines and their IC₅₀ values were determined. To test their selectivity potential for tumour cells, three of the most potent benzofuran derivatives (**4b**, **15a**, and **16a**) were selected to be evaluated for their cytotoxic activity against non-tumorigenic human lung WI-38. Moreover, in the aim of exploring the mechanistic antiproliferative activity of the tested molecules at the molecular level, the three most potent molecules were evaluated for their VEGFR-2 inhibitory activity. In addition, the three most potent antiproliferative compounds (**4b**, **15a**, and **16a**) were tested for their antitubercular activity. Finally, cell cycle analysis studies were conducted, including apoptosis assay and Annexin V-FITC assay.

2. Results and discussion

2.1. Chemistry

Preparation of target 3-methylbenzofurans (**4a-d**, **6a-c**, **8a-c** and **11**) and 3-(morpholinomethyl)benzofurans (**15a-c**, **16a-b**, **17a-b** and **18**) are depicted in Schemes 1–4.

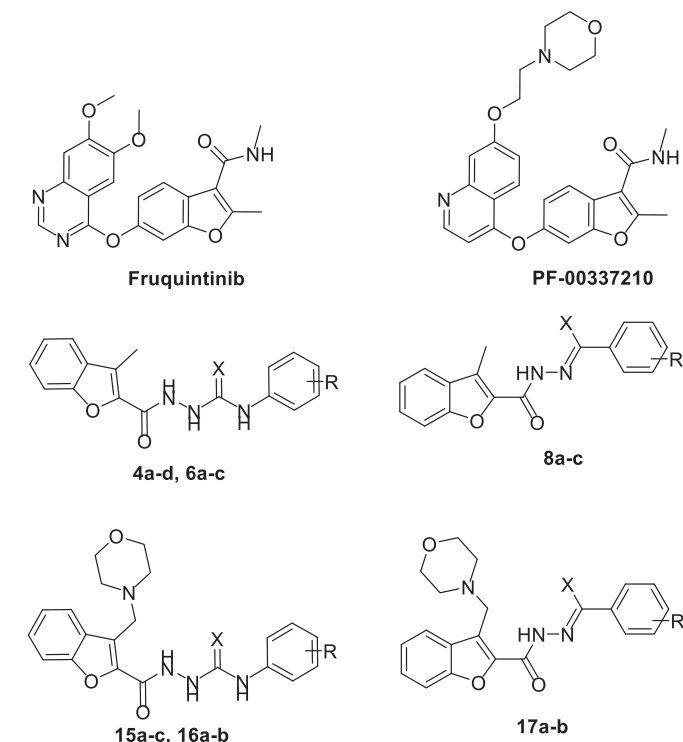
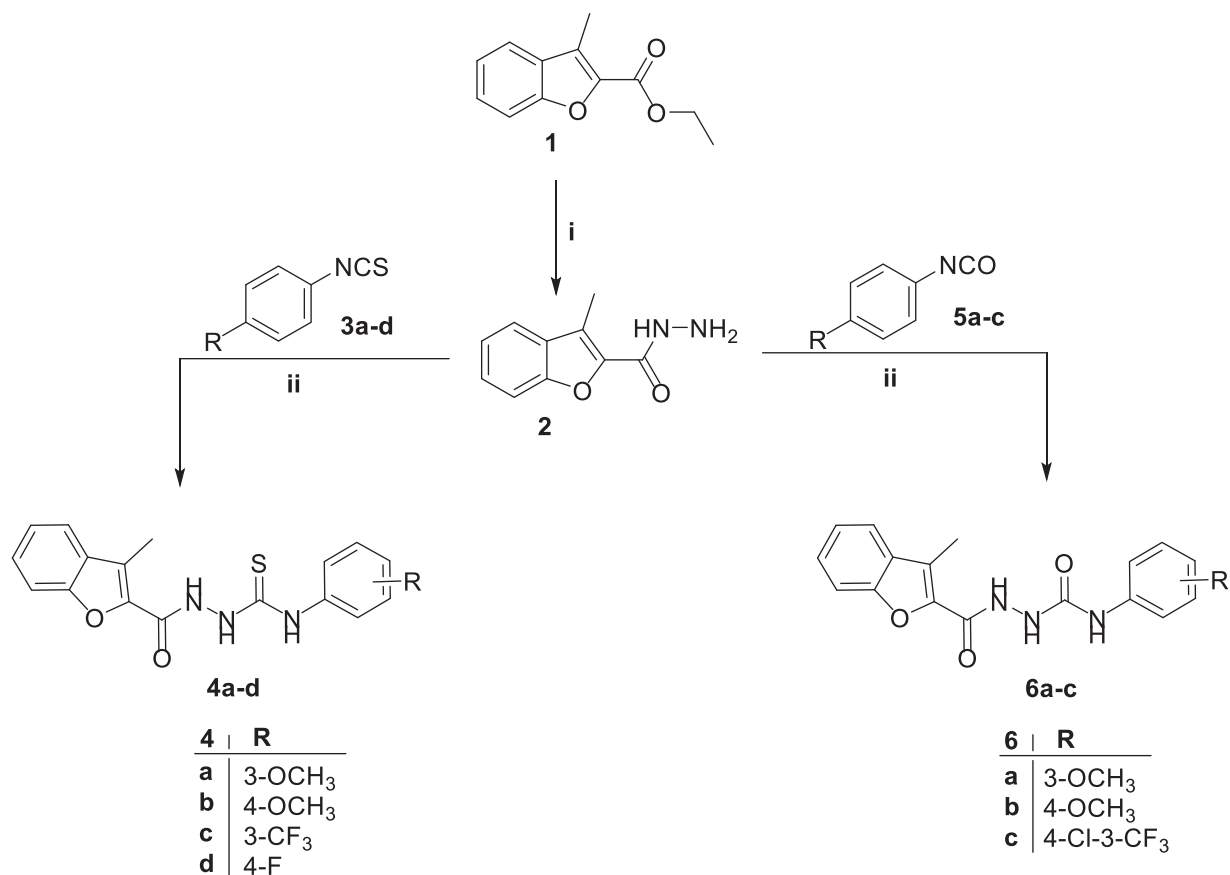
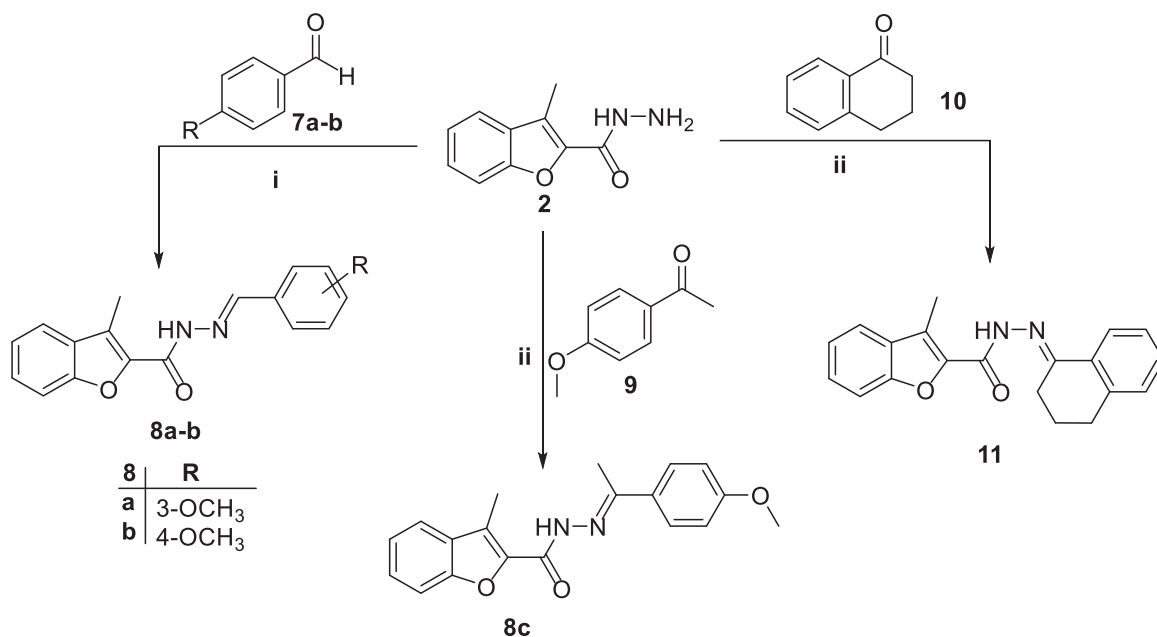


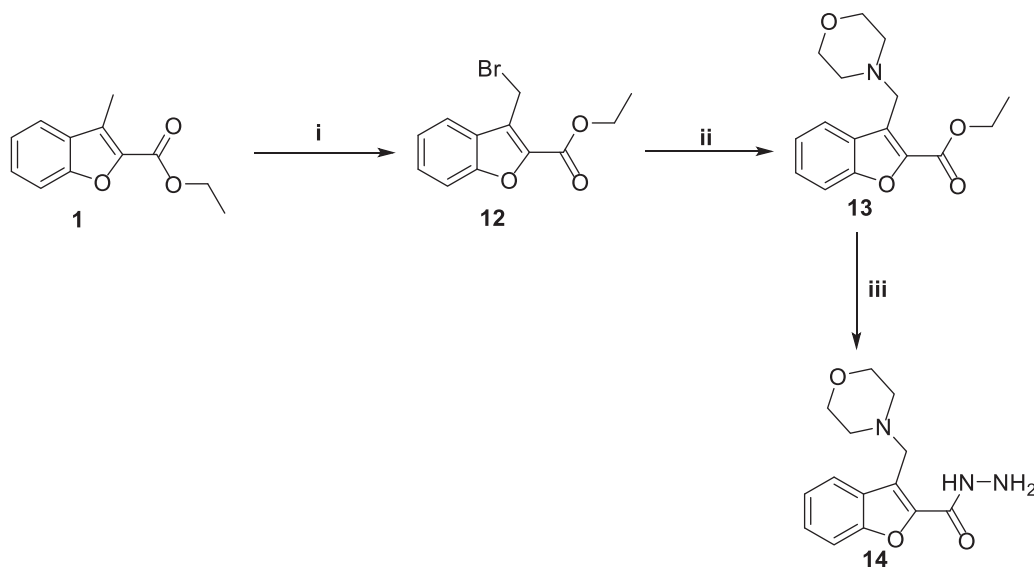
Figure 1. Chemical structures of benzofurans Fruquintinib and PF-00337210, as well as structures of target 2-methylbenzofurans (**4a-d**, **6a-c** and **8a-c**) and 3-(morpholinomethyl)benzofurans (**15a-c**, **16a-b** and **17a-b**).



Scheme 1. Synthesis of target 2-methylbenzofurans **4a-d** and **6a-c**; reagents and conditions: (i) NH₂NH₂·H₂O/isopropyl alcohol/reflux 2 h and (ii) dry toluene/reflux 7 h.



Scheme 2. Synthesis of target 2-methylbenzofurans **8a–c** and **11**; reagents and conditions: (i) Ethanol/Cat. Acetic acid/reflux 3 h, (ii) ethanol/cat. Acetic acid/reflux 7 h.

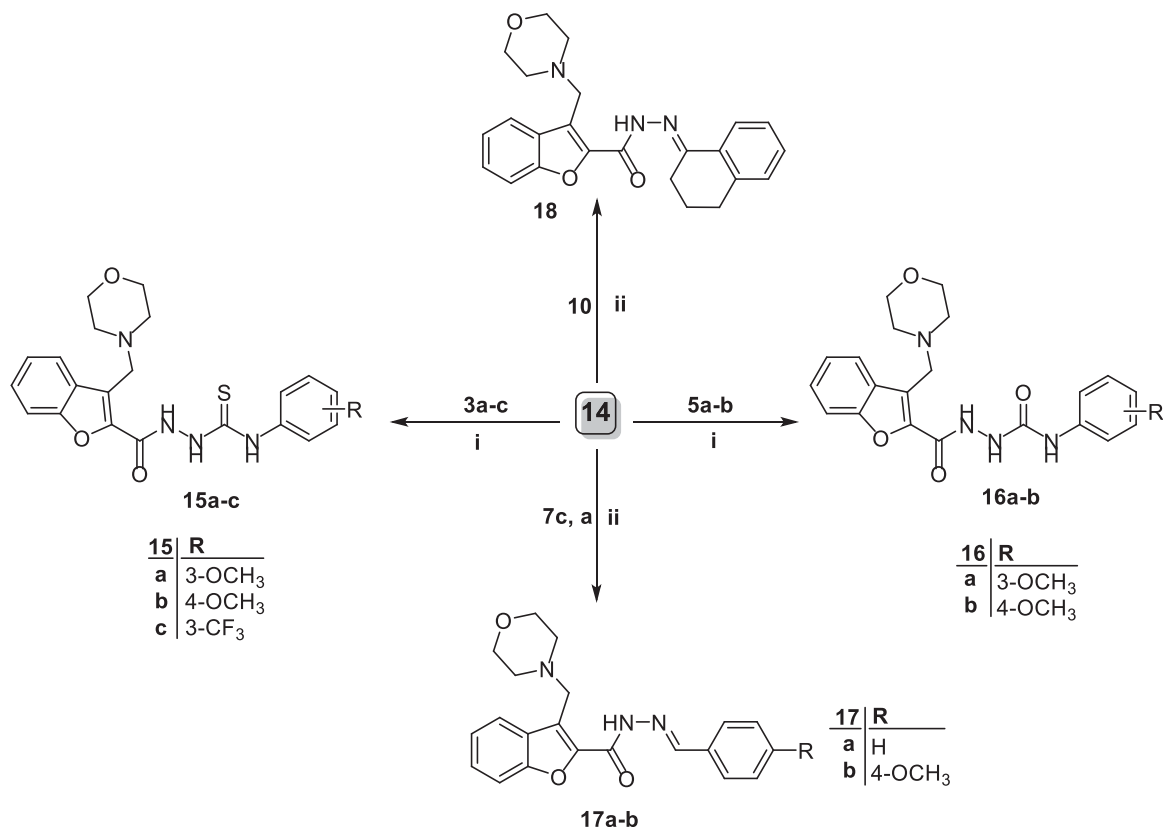


Scheme 3. Synthesis of key intermediate 3-(morpholinomethyl)benzofuran-2-carbohydrazide **14**; Reagents and conditions: (i) NBS/carbon tetrachloride/dibenzoyl peroxide/reflux 16 h, (ii) Morpholine/Acetonitrile/K₂CO₃/KI/reflux 8 h, and (iii) NH₂NH₂·H₂O/isopropyl alcohol/reflux 2 h.

First, 3-methylbenzofuran-2-carbohydrazide **2** was prepared from its precursor ethyl 3-methylbenzofuran-2-carboxylate **1** by nucleophilic substitution reaction using hydrazine hydrate as a nucleophile. Then, upon reacting hydrazide **2** with isothiocyanates **3a–d** and isocyanates **5a–c** in anhydrous toluene, only the more nucleophilic N₂ adds to the C=N double bond of either **3a–d** or **5a–c** to afford the desired 1-acylatedthiosemicarbazides (**4a–d**) and 1-acylatedsemicarbazides (**6a–c**), respectively (Scheme 1).

Furthermore, the key intermediate 3-methylbenzofuran-2-carbohydrazide **2** underwent a nucleophilic addition–elimination reaction with the carbonyl group of aldehydes **7a–b** as well as ketones **9** and **10** to afford aldohydrazone **8a–b** and ketohydrazone **8c** and **11**, respectively. This condensation reaction was carried out in refluxing ethanol with presence of catalytic drops of acetic acid (Scheme 2).

On the other hand, *N*-bromosuccinimide (NBS) reagent was utilized to selectively brominate the reactive benzofuran-3-ylmethyl group, in a mild bromination step, affording ethyl 3-(bromomethyl)benzofuran-2-carboxylate **12**. Thereafter, a nucleophilic substitution reaction at the bromomethyl carbon of compound **12** was carried out by morpholine and was triggered by nucleophilic assistance with iodide ion to furnish ethyl 3-(morpholinomethyl)benzofuran-2-carboxylate **13**. The soft iodide nucleophile would selectively attack the soft electrophilic bromomethyl carbon rather than the harder one (i.e. the ester in this case) according to the HSAB theory³³. Such nucleophilic assistance exerted by iodide ion enhances the reactivity of the 3-methylene group *via* enhancement of the leaving group ability by replacing a quite good leaving group (i.e. bromide) with a better one (iodide). The next step was quite similar to the preparation of hydrazide **2**, in this step,



Scheme 4. Synthesis of target 3-(morpholinomethyl)benzofurans **15–18**; reagents and conditions: (i) dry toluene/reflux 7 h and (ii) ethanol/cat. Acetic acid/reflux 3 h.

the 3-(morpholinomethyl)benzofuran-2-carboxylate ester **13** was treated with hydrazine hydrate in refluxing ethanol to afford the desired hydrazide **14** (Scheme 3).

Finally, target 1-acylatedthiosemicarbazides (**15a–c**), 1-acylated-semicarbazides (**16a,b**) and aldehydrazones **17a–b** and ketohydrazones **18** were prepared through reaction of 3-(morpholinomethyl)benzofuran-2-carbohydrazide **14** with different isothiocyanatobenzene **3a–d**, isocyanatobenzene **5a–c** and carbonyl moieties **7a,c** and **10**, Scheme 4.

2.2. Biological evaluation

2.2.1. Anti-proliferative activity towards non-small cell lung carcinoma A549 and NCI-H23 cell lines

The antiproliferative activity of the synthesised derivatives of the 3-methylbenzofuran series (**4a–d**, **6a–c**, **8a–c** and **11**) and the 3-(morpholinomethyl)benzofuran series (**15a–c**, **16a–b**, **17a–b** and **18**) was evaluated against non-small cell lung carcinoma (NSCLC) A549 and NCI-H23 cell lines, following the procedures of the MTT assay³⁴. The antiproliferative activity of the 3-methylbenzofuran derivatives (**4a–d**, **6a–c**, **8a–c** and **11**) against A549 cancer cell line ranges from 47.02 μM down to 1.48 μM . Superiorly, 3-methylbenzofuran derivative **4c**, with a *para*-methoxy group grafted on the terminal phenyl ring, showed the highest antiproliferative activity ($\text{IC}_{50} = 1.48 \mu\text{M}$) which is comparable to staurosporine ($\text{IC}_{50} = 1.52 \mu\text{M}$), Table 1. Whereas, the antiproliferative potency of the 3-(morpholinomethyl)benzofurans (**15a–c**, **16a–b**, **17a–b** and **18**) showed narrower range of activity against the same cell line with IC_{50} values ranging from 18.89 μM down to 1.5 μM , which verifies that substitution of the benzofuran ring by a methyl morpholino group boosts the cytotoxic activity against cell line lung carcinoma A549. The most potent compound **16a**, bearing a 3-

Table 1. Cytotoxic impact against non-tumorigenic human lung WI-38 cell line, as well as mean tumour selectivity index (S.I.) (WI-38/A549 and NCI-H23).

Compounds	IC_{50} (μM)			Mean tumour selectivity
	WI-38	A549	NCI-H23	
4b	19.51 ± 1.18	1.48 ± 0.08	5.90 ± 0.29	5.3
15a	32.81 ± 1.98	5.27 ± 0.29	2.52 ± 0.13	8.4
16a	12.86 ± 0.78	1.50 ± 0.08	0.49 ± 0.02	12.9

methoxy group substituted on the phenyl ring, exhibited antiproliferative activity which is equivalent to that recorded by staurosporine ($\text{IC}_{50} = 1.52 \mu\text{M}$ and $1.50 \mu\text{M}$, respectively).

Alternatively, evaluating the antiproliferative activity of the synthesised compounds against NCI-H23 cancer cell line reveals that all the compounds showed lower antiproliferative activity evident by their higher IC_{50} values. The IC_{50} values of the 3-methylbenzofuran series (**4a–d**, **6a–c**, **8a–c** and **11**) range from 67.22 μM down to 5.90 μM which is much higher than those values recorded against A549 cancer cell line (47.02 μM –1.48 μM).

Controversially, the IC_{50} values of 3-(morpholinomethyl)benzofuran series (**15a–c**, **16a–b**, **17a–b** and **18**) demonstrated more potent antiproliferative activity against NCI-H23 cancer cell line which ranges from 29.75 μM down to 0.49 μM with the exception of compound **15b** that possessed poor antiproliferative activity with an IC_{50} value of 68.9 μM . These results again reinforces the previously observed antiproliferative activity which supports the conclusion that substituting the benzofuran ring with a methyl morpholino group is advantageous for the cytotoxic activity against both tested lung cancer cell lines; A549 and NCI-H23. Interestingly, compound **16a** with a 3-methoxy group proved to be the most potent compound with 2.53 fold more potent as compared to staurosporine. Moreover, **15a** ($\text{IC}_{50} = 2.52 \mu\text{M}$) and **15c** ($\text{IC}_{50} = 2.218 \mu\text{M}$) exhibited excellent antiproliferative activity as compared to staurosporine ($\text{IC}_{50} = 1.24 \mu\text{M}$).

2.2.2. Cell cycle analysis

To understand the underlying mechanism of the tumour suppression activity of the tested benzofurans, the three most active compounds in this study, **4b**, **15a** and **16a** were further investigated for their effects on the cell cycle progression in A549 (for **4b**) and NCI-H23 (for **15a** and **16a**) cancer cell lines.

Analysing the results for the three benzofurans on the two investigated cell lines revealed that they affected the cell cycle progression in a similar manner, where **4b**, **15a** and **16a** reduced the G0–G1 phase by 0.67-, 0.56- and 0.47-folds, respectively. Moreover, the S phase was also attenuated by 0.46, 0.50 and 0.51 fold, respectively. This reduction was accompanied by augmentation of the cell population in the G2/M phase by 2.67-, 5.33- and

6.90-fold, respectively, and in the sub-G1 phase by 21.76-, 13.13- and 12.54-fold, respectively, as compared to the control (Figure 2).

2.2.3. Apoptosis assay

The apoptotic effect of the three benzofurans (**4b**, **15a** and **16a**) was evaluated using Annexin V-FITC/PI (AV/PI) dual staining assay to validate if their observed cytotoxic effect is due to non-specific necrosis or physiological apoptosis. The apoptotic effect of 3-methylbenzofuran derivative **4b** was observed against A549 cell line using a control, where **4b** affected 42.05% of apoptosis compared to that triggered by control which was 1.37% (Figure 3). Moreover, the apoptotic effects of 3-(morpholinomethyl)benzofuran derivatives **15a** and **16a** were evaluated in NCI-H23 cancer

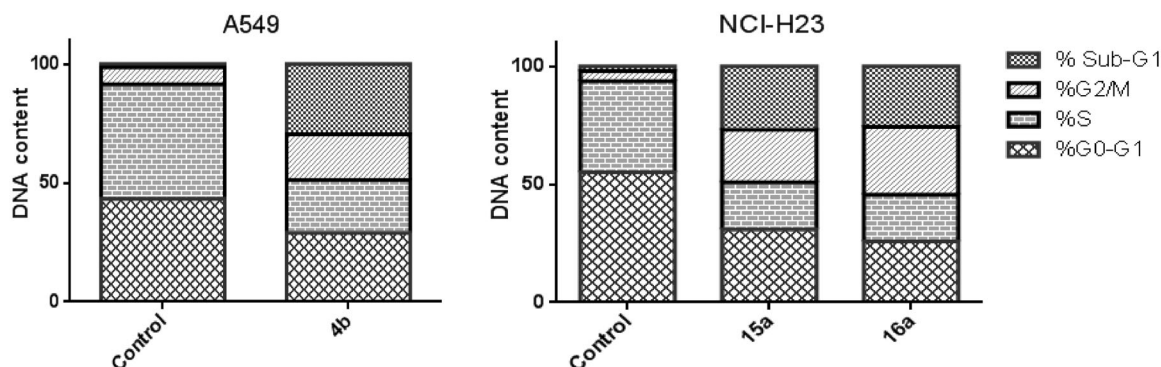


Figure 2. Effect of 3-methylbenzofuran derivative **4b** on the phases of cell cycle of A549 cells, and effect of 3-(morpholinomethyl)benzofuran derivatives **15a** and **16a** on the phases of cell cycle of NCI-H23 cells.

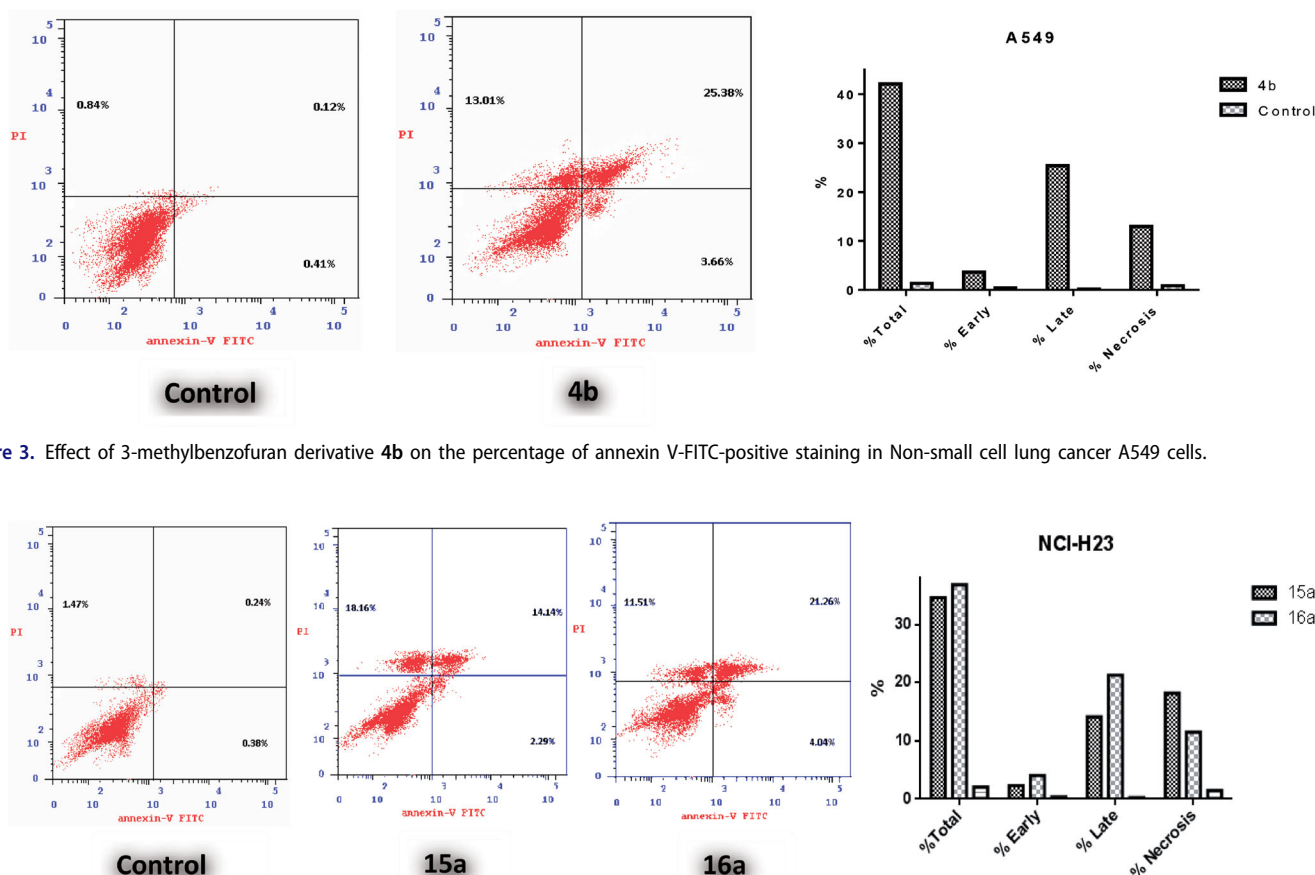


Figure 3. Effect of 3-methylbenzofuran derivative **4b** on the percentage of annexin V-FITC-positive staining in Non-small cell lung cancer A549 cells.

Figure 4. Effect of 3-(morpholinomethyl)benzofuran derivatives **15a** and **16a** on the percentage of annexin V-FITC-positive staining in Non-small cell lung cancer NCI-H23 cells.

cell line. Results revealed that benzofuran **15a** produced 34.59% of total apoptosis, as well as, benzofuran **16a** caused 36.81% of total apoptosis compared to the control which produced only 2.09% of total apoptosis (Figure 4). Based on the previous results, compounds **4b**, **15a** and **16a** proved to induce apoptosis significantly in both cancer cell lines; A-549 and NCI-H23.

2.2.4. Cytotoxic activity against non-tumorigenic human lung WI-38 cell line

Antiproliferative agents are designed to inhibit the cellular growth of tumour cells selectively, while sparing the normal cells. Accordingly, the three most potent benzofurans; **4b**, **15a** and **16a** were evaluated for their cytotoxic activity against non-tumorigenic human lung WI-38 cell line and their IC_{50} values were compared to those detected against the lung cancer cell lines A549 and NCI-H23 (Table 2).

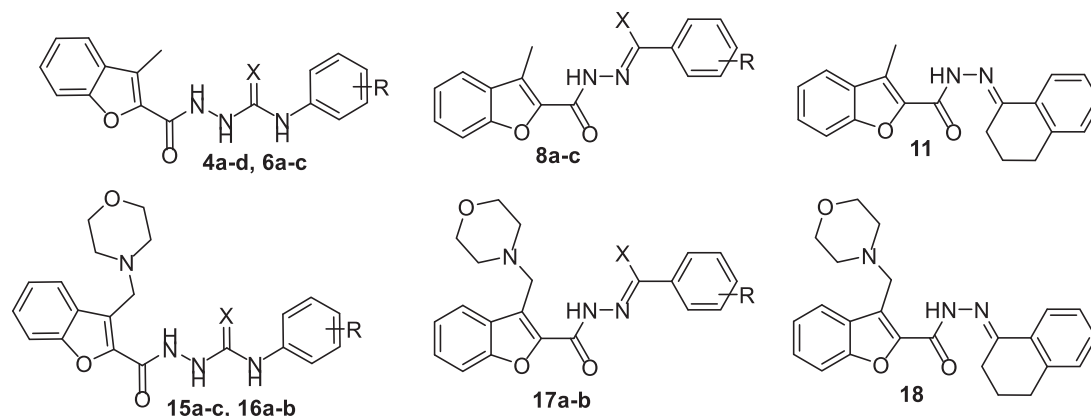
Scrutinising the results revealed that the three tested benzofurans are barely toxic to the non-tumorigenic human lung WI-38 cell line with high IC_{50} values of 19.51 μ M, 32.81 μ M and 12.86 μ M, respectively (Table 2). On the other hand, they exhibited marked antiproliferative activity against the lung cancer cell lines A549 and NCI-H23 with much lower IC_{50} values of 1.48 μ M, 5.27 μ M and 1.5 μ M for A549 cancer cell line, and 5.90 μ M, 2.52 μ M and 0.49 μ M for NCI-H23 cancer cell line, respectively (Table 2). A much more

indicative parameter for the relative safety of the three tested compounds is the mean tumour selectivity value which was calculated for the three compounds to be 5.3, 8.4 and 12.9, respectively. These values prove that the three tested benzofurans exhibited selective antiproliferative activity against tumour cells while sparing the normal cells.

2.2.5. VEGFR-2 inhibitory assay

Surveying the literature revealed that VEGFR-2 inhibition is one of the well-known reported antiproliferative mechanisms of benzofuran-based small molecules^{24–26,29–32}. Accordingly, the potential VEGFR-2 inhibitory activity of the three most potent molecules; **4b**, **15a** and **16a** were evaluated in the aim of exploring the cellular proliferation inhibitory potential of the tested compounds at the molecular level. Interestingly, results revealed that all of the three tested benzofurans (**4b**, **15a** and **16a**) exhibited excellent inhibition of VEGFR-2 at nanomolar range with IC_{50} values of 77.97 nM, 132.5 nM and 45.4 nM, although none of them was superior to sorafenib (IC_{50} = 34.68 nM) (Table 3). This suggests that the herein reported benzofurans exert their antiproliferative activity by inhibition of VEGFR-2 resulting in inhibition of angiogenesis and ultimately cell death.

Table 2. *In vitro* anti-proliferative activity of target 3-methylbenzofurans (**4a–d**, **6a–c**, **8a–c** and **11**) and 3-(morpholinomethyl)benzofurans (**15a–c**, **16a–b**, **17a–b** and **18**) against lung A549 and NCI-H23 cancer cell lines.



Compounds	X	R	IC_{50} (μ M) ^a	
			A549	NCI-H23
4a	S	3-OCH ₃	10.09 \pm 0.55	34.18 \pm 1.71
4b	S	4-OCH ₃	1.48 \pm 0.08	5.90 \pm 0.29
4c	S	3-CF ₃	36.49 \pm 0.2	24.36 \pm 0.12
4d	S	4-F	12.79 \pm 0.7	67.22 \pm 3.36
6a	O	3-OCH ₃	15.11 \pm 0.83	56.66 \pm 2.83
6b	O	4-OCH ₃	12.5 \pm 0.68	9.24 \pm 0.46
6c	O	4-Cl-3-CF ₃	47.02 \pm 2.57	24.54 \pm 1.23
8a	H	3-OCH ₃	44.1 \pm 2.41	14.89 \pm 0.74
8b	H	4-OCH ₃	9.204 \pm 0.5	6.148 \pm 0.31
8c	CH ₃	4-OCH ₃	16.35 \pm 0.89	13.95 \pm 0.7
11	–	–	30.19 \pm 1.65	12.05 \pm 0.6
15a	S	3-OCH ₃	5.273 \pm 0.29	2.525 \pm 0.13
15b	S	4-OCH ₃	5.7 \pm 0.31	68.9 \pm 3.44
15c	S	3-CF ₃	6.303 \pm 0.34	2.218 \pm 0.11
16a	O	3-OCH ₃	1.50 \pm 0.08	0.49 \pm 0.02
16b	O	4-OCH ₃	18.89 \pm 1.03	5.089 \pm 0.25
17a	H	H	6.01 \pm 0.03	22.97 \pm 1.15
17b	H	4-OCH ₃	10.83 \pm 0.59	3.043 \pm 0.15
18	–	–	3.697 \pm 0.2	29.75 \pm 1.49
Staurosporine	–	–	1.52 \pm 0.05	1.24 \pm 0.02

^a IC_{50} values are the mean \pm SD of three separate experiments.

Table 3. Inhibitory activity of target benzofurans **4b**, **15a** and **16a** against VEGFR-2.

Compounds	IC ₅₀ (nM) VEGFR-2
4b	77.97 ± 4.6
15a	132.5 ± 7.8
16a	45.4 ± 2.7
Sorafenib	34.68 ± 2.6

Table 4. Anti-tubercular activity of the target compounds **4b**, **15a** and **16a**.

Compounds	MIC (μg/ml)
4b	500
15a	62.5
16a	125
INH	0.24

Table 5. The detailed bonding interactions and binding scores for the benzofurans **4b**, **15a** and **16a**.

Compounds	Score kcal/mole	Bonding interaction	Distance (Å)
4b	−9.9	Hydrogen bond with GLU885	2.66
		Hydrogen bond with CYS1045	2.38
		Hydrogen bond with ASP1046	3.05
		Pi-alkyl with LEU889	5.37
		Pi-anion with ASP1046	4.88
		Pi-donor with ASP1046	2.67
		Pi-alkyl with LYS868	5.41
		Pi-alkyl with CYS1045	4.17
		Pi-Pi interaction with PHE1047	4.91
		Pi-lone pair with PHE1047	2.68
15a	−10.4	Hydrogen bond with GLU885	2.88
		Hydrogen bond with CYS1045	2.47
		Hydrogen bond with ASP1046	2.58
		Pi-alkyl with LEU889	5.33
		Alkyl-alkyl with VAL898	5.13
		Alkyl-alkyl with LEU1019	4.57
		Alkyl-alkyl with ILE1044	5.04
		Pi-alkyl with HIS1026	5.46
		Pi-alkyl with LYS868	5.34
		Pi-alkyl with CYS1045	4.33
		Pi-Pi interaction with PHE1047	4.66
		Pi-lone pair with PHE1047	2.29
		Hydrogen bond with GLU885	2.87
		Hydrogen bond with CYS1045	2.47
16a	−10.5	Hydrogen bond with ASP1046	2.93
		Pi-alkyl with LEU889	5.33
		Pi-alkyl with ILE888	5.25
		Alkyl-alkyl with VAL898	5.18
		Alkyl-alkyl with LEU1019	4.54
		Alkyl-alkyl with ILE1044	5.04
		Pi-alkyl with HIS1026	5.40
		Pi-alkyl with LYS868	5.48
		Pi-alkyl with CYS1045	4.07
		Pi-Pi interaction with PHE1047	4.79
		Pi-lone pair with PHE1047	2.29

2.2. Anti-tubercular activity

Lung infections, headed by tuberculosis have been implicated as potentially contributing to lung cancer³⁵. In this study, we decided to explore the potential anti-tubercular activity of target benzofuran derivatives¹⁷. The three most promising benzofuran-based derivatives herein reported (**4b**, **15a** and **16a**) were assessed for their potential anti-tubercular activity towards *M. tuberculosis* following the procedures of the Microplate Alamar Blue Assay³⁶, and using INH as a reference anti-TB drug. The results are expressed as minimum inhibitory concentration and presented in Table 4.

The results of the Microplate Alamar Blue assay highlighted that the tested benzofuran derivatives (**4b**, **15a** and **16a**) exerted

moderate to weak anti-tubercular activity. The 3-(morpholinomethyl)benzofuran derivatives **15a** and **16a** revealed moderate activity with MIC values equal 62.5 and 125 μg/ml, respectively, whereas the 3-methylbenzofuran derivative **4b** showed high MIC value equals 250 μg/ml (Table 4).

2.4. Docking studies

This section aimed to predict the plausible binding mode of target benzofuran-based small molecules herein reported with VEGFR-2 binding site, as well as correlating the retrieved biological activities with binding poses to establish guidance for future optimisation of the lead compounds. As it is an error prone technique, molecular docking is to be validated by comparison to an experimental reference; accordingly the co-crystallized Sorafenib was re-docked to its VEGFR-2 active site (PDB: 4ASD³⁷) where the calculated RMSD values between the co-crystallized Sorafenib and docked poses were 0.71 Å (Supporting materials, Figure S1). Also, the re-docking validation perfectly reproduced all original interactions between the co-crystallized Sorafenib and the VEGFR-2 active site.

The examined benzofuran derivatives (**4b**, **15a** and **16a**) achieved favourable interaction pattern and good binding affinities ($S = -9.9$, -10.5 and -10.4 kcal/mole, Table 5) within their VEGFR-2, in comparison to the reference Sorafenib that achieved a score of -11.1 kcal/mole. In details, benzofuran derivatives **4b**, **15a** and **16a** were successfully engaged in many types of hydrophobic and hydrogen bonding interactions. Of particular importance, the three benzofurans were engaged in two hydrogen bonding interactions through their NH and carbonyl oxygen (C=O) functionalities of the hydrazide linker with the key GLU-885 and ASP-1046 amino acids residues, respectively (Figures 5–7). In addition, the oxygen of the grafted methoxy group on the terminal phenyl moieties acted as HBA and achieved a third hydrogen bond interaction with CYS-1045, Figures 5–7.

Furthermore, the appended morpholine moiety in benzofurans **15a** and **16a** was able to form various hydrophobic interactions with non-polar residues such as VAL-898, LEU-1019 and ILE-1044, which should explain the higher energy score achieved by compounds **15a** and **16a** than compound **4b** that lacks the morpholine moiety, Figures 5–7. Table 5 summarises the bonding interactions between benzofurans **4b**, **15a** and **16a** and VEGFR-2 binding site.

3. Conclusions

The current study presented the synthesis and *in vitro* biological assessment of two sets of 3-methylbenzofurans (**4a–d**, **6a–c**, **8a–c** and **11**) and 3-(morpholinomethyl)benzofurans (**15a–c**, **16a–b**, **17a–b** and **18**) as potential anticancer agents towards non-small cell lung carcinoma A549 and NCI-H23 cell lines, with VEGFR-2 inhibitory activity. The 3-methylbenzofuran counterparts **4c**, with a *para*-methoxy group grafted on the terminal phenyl ring, exerted the best antiproliferative activity against A549 cell line (IC₅₀ = 1.48 μM) which is comparable to staurosporine (IC₅₀ = 1.52 μM), whereas the 3-(morpholinomethyl)benzofurans **15a**, **15c** and **16a** displayed excellent activity against NCI-H23 cell line (IC₅₀ = 2.52, 2.21 and 0.49 μM). Benzofurans (**4b**, **15a** and **16a**) were further investigated for their effects on the cell cycle progression and apoptosis in A549 (for **4b**) and NCI-H23 (for **15a** and **16a**) cell lines. The examined compounds significantly affected the cell cycle progression and provoked apoptosis within the tested cell lines. Furthermore, benzofurans **4b**, **15a** and **16a** displayed

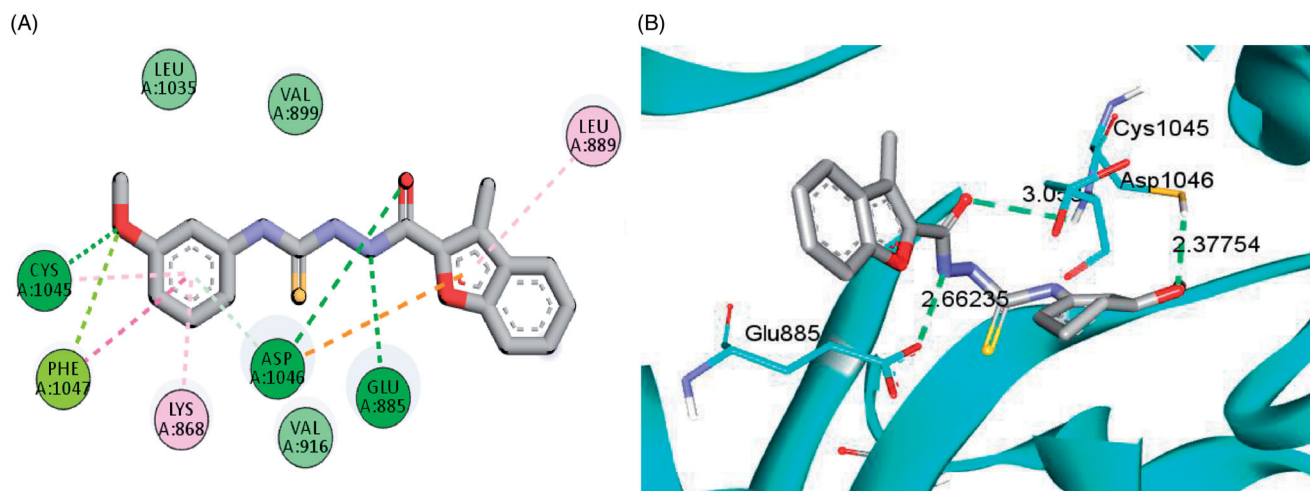


Figure 5. 2D (A) and 3D (B) interactions of 3-methylbenzofuran derivative **4b** within VEGFR-2 binding site (PDB: 4ASD).

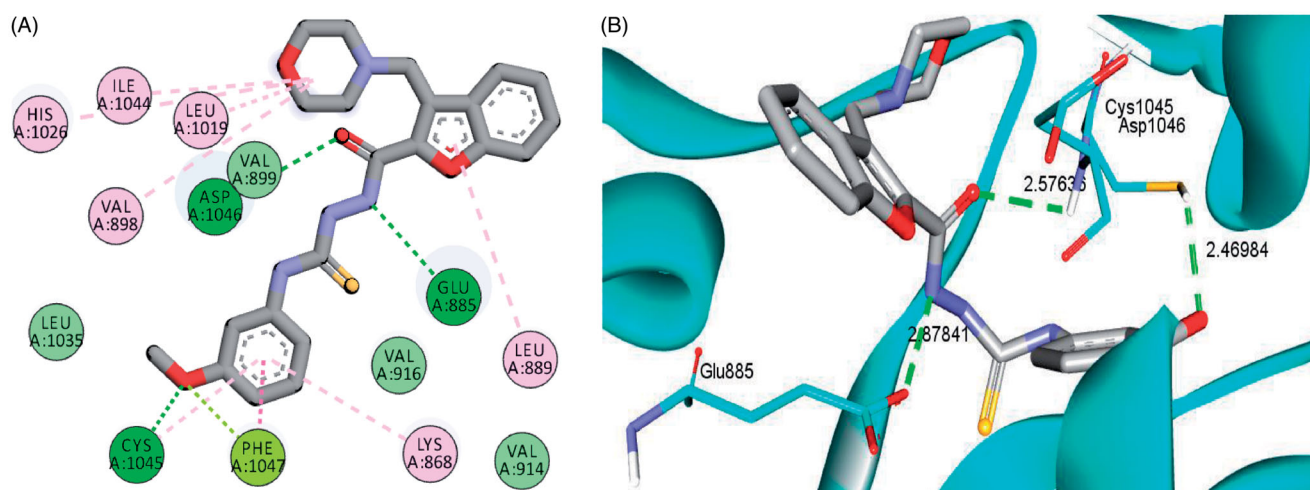


Figure 6. 2D (A) and 3D (B) interactions of 3-(morpholinomethyl)benzofuran derivative **15a** within VEGFR-2 binding site (PDB: 4ASD).

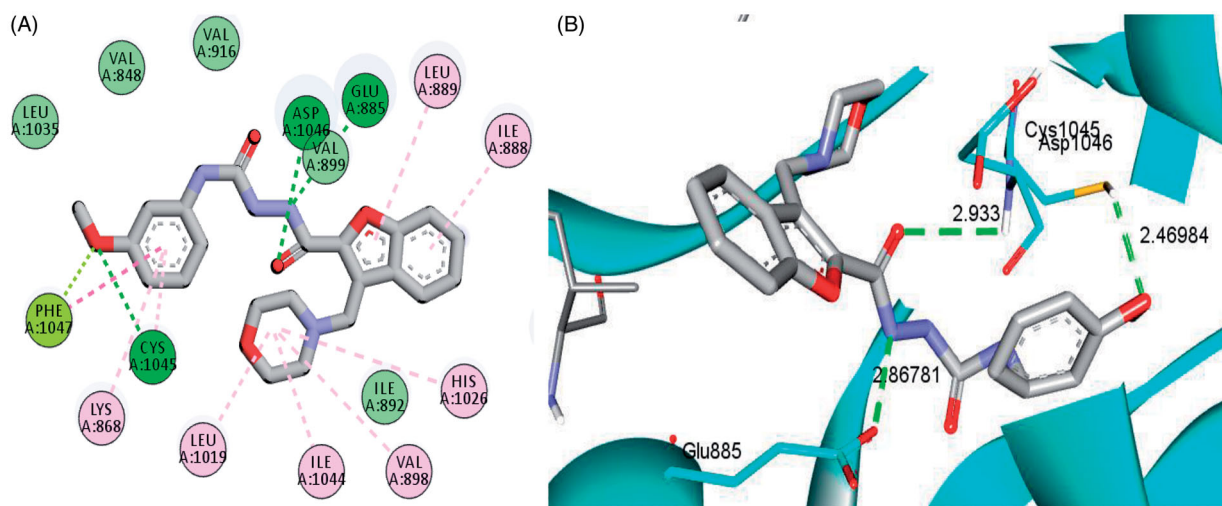


Figure 7. 2D (A) and 3D (B) interactions of 3-(morpholinomethyl)benzofuran derivative **16a** within VEGFR-2 binding site (PDB: 4ASD).

good VEGFR-2 inhibitory activity with an IC_{50} value equal to 77.97, 132.5 and 45.4 nM, respectively. In addition, the cytotoxic impact of the three benzofurans was assessed towards normal lung WI-38 cells, where they elicited a mean tumour selectivity values equal

5.3, 8.4 and 12.9, respectively. The conducted molecular docking study highlighted that benzofuran derivatives **4b**, **15a** and **16a** were successfully engaged in many types of hydrophobic and hydrogen bonding interactions. Of particular importance, they

were engaged in two hydrogen bonding interactions through their NH and carbonyl oxygen (C=O) functionalities of the hydrazide linker with the key GLU-885 and ASP-1046 amino acids residues, respectively, whereas, the oxygen of the grafted methoxy group achieved a third hydrogen bond interaction with CYS-1045.

4. Experimental

4.1. Chemistry

Solvents used were of HPLC grade and purchased from Sigma-Aldrich (Chicago, IL). Reaction follow up was carried out using pre-coated F₂₅₄ Merck TLC plates (Kenilworth, NJ). Shimadzu FT-IR spectrometer (Shimadzu, Kyoto, Japan) was used for functional group analysis of the synthesised compounds. NMR spectrometric analyses were carried out using Bruker-Avance 400 NMR spectrometer (100 MHz for ¹³C- and 400 MHz for ¹H-NMR experiments, respectively). Chemical shifts were recorded in ppm after setting standard solvent signals (DMSO-d₆ at δ : 2.54 ppm for ¹H- and δ : 40.45 ppm for ¹³C NMR spectra). Multiplicities were reported with their first-order J coupling constants (Hz) for doublets (d); triplets (t); quartets (q) as well as second-order J constants (whenever possible) for the second-order splitting (e.g. doublet of triplets dt). Stuart apparatus was used for determination of melting points. FLASH 2000 CHNS/O analyser was utilised for performing elemental analysis. Compounds **1** and **2**²³, and **12**³⁸ were previously reported.

4.1.2. Preparation of ethyl 3-(morpholinomethyl)benzofuran-2-carboxylate (**13**)

Compound **13** was prepared by refluxing ethyl 3-(bromomethyl)-benzofuran-2-carboxylate **12** (1.98 g, 7 mmol) in acetonitrile with an excess of morpholine (1.31 g, 15 mmol) using anhydrous potassium carbonate as a base. The reaction completion was followed up by TLC. After consumption of the ester **12**, the inorganic salts were filtered off. Then, the solvent was evaporated and the residue recrystallized from ether-DCM (3:1) giving the desired product as white powder; yield (1.56 g 77%). This product was used in the next step for synthesis of hydrazide **14** without further purification.

4.1.3. General method for preparation of hydrazides **2** and **14**

The appropriate ester **1** or **13** (4 mmol) was dissolved in absolute isopropyl alcohol (12 ml). Then, (1 g, 20 mmol) of 99% hydrazine hydrate was drop-wise added before the whole mixture was refluxed for 2 h. Solvent and most reagents were then distilled off, and the residue washed several times with water. Crystallisation from ethanol 85% afforded the final crystalline hydrazide.

4.1.3.1. 3-Methylbenzofuran-2-carbohydrazide (2**)**. White crystals, mp = 138–140 °C (reported mp = 135 °C³⁸), yield = 75%.

4.1.3.2. 3-(Morpholinomethyl)benzofuran-2-carbohydrazide (14**)**. White crystals, mp = 207–209 °C, yield 70%; ¹H NMR (400 MHz, DMSO-d₆) δ : 10.45 (s, NH, 1H), 7.90 (d, H-4 of benzofuran, J = 8.0 Hz, 1H), 7.60 (d, H-7 of benzofuran, J = 8.0 Hz, 1H), 7.43 (t, H-6 of benzofuran, J = 8.0 Hz, 1H), 7.32 (t, H-5 of benzofuran, J = 7.2 Hz, 1H), 4.62 (s, 2H, NH₂), 3.97 (s, 2H, -CH₂-morpholine), 3.58 (s, 4H, CH₂OCH₂ of morpholinyl moiety), 2.51 (s, 4H, CH₂NCH₂ of morpholinyl moiety). ¹³C NMR (100 MHz, DMSO-d₆) 158.84 (C=O), 153.44, 145.47, 128.88, 127.19, 123.79, 122.26, 119.59,

112.06, 66.63 (O(CH₂)₂), 53.25 (N(CH₂)₂), 51.01 (CH₂). Anal. Calcd. for C₁₄H₁₇N₃O₃ (275.31): C, 61.08; H, 6.22; N, 15.26; Found: C, 60.84; H, 6.25; N, 15.33.

4.1.4. General method for the synthesis of thiosemicarbazides **4a–d**, **15a–c** and semicarbazides **6a–c**, **16a,b**

The proper isocyanate or isothiocyanate derivative (0.7 mmol) was dissolved in 5 ml of stirred dry toluene. Similarly, a solution of the proper hydrazide **2** or **14** (0.6 mmol) in 3 ml of hot stirred toluene/dioxane solvent mixture (5:1, respectively) was prepared. To this latter solution was dropwise added the isocyanate or isothiocyanate solution in toluene, and then the reaction mixture was refluxed for 7 h. The absence of the TLC spot of the starting hydrazide was safely considered a sign of the reaction coming to an end. After that, the precipitate formed upon cooling was filtered off, dried by suction, washed with toluene (3 × 4 ml), dried again in hot air oven for 5 h at 90 °C. Further recrystallization from dioxane-toluene mixture affords the desired thiosemicarbazides **4a–d**, **15a–c** and semicarbazides **6a–c**, **16a,b** in good yield.

4.1.4.1. N-(3-Methoxyphenyl)-2-(3-methylbenzofuran-2-carbonyl)-hydrazine-1-carbothioamide (4a**)**. White crystals, mp = 172–174 °C, yield 80%; IR (cm⁻¹): 3484 (br, NH groups), 1653 (C=O hydrazide), 1276 (C=S thiosemicarbazide). ¹H NMR (400 MHz, DMSO-d₆) δ : 2.61 (s, CH₃ C-3 of benzofuran, 3H), 3.77 (s, OCH₃, 3H), 6.77 (d, H-4 of 3-CH₃OC₆H₄-, J = 8.1 Hz, 1H), 7.11 (d, H-6 of 3-CH₃OC₆H₄-, J = 7.9 Hz, 1H), 7.22 (s, H-2 of 3-CH₃OC₆H₄-, 1H), 7.26 (t, H-5 of 3-CH₃OC₆H₄-, J = 8.1 Hz, 1H), 7.41 (t, H-5 of benzofuran, J = 7.4 Hz, 1H), 7.55 (t, H-6 of benzofuran, J = 7.7 Hz, 1H), 7.66 (d, H-7 of benzofuran, J = 8.3 Hz, 1H), 7.82 (d, H-4 of benzofuran, J = 7.8 Hz, 1H), 9.79 (s, NH, 2H), 10.65 (s, NH, 1H). ¹³C NMR (100 MHz, DMSO-d₆) 181.29 (C=S), 159.76 (C=O), 153.3, 142.54, 140.82, 129.35, 129.14, 128.02, 123.8, 122.85, 121.66, 118.19, 112.13, 111.77, 110.83, 55.56 (OCH₃), 9.27 (CH₃). Anal. Calcd. for C₁₈H₁₇N₃O₃S (355.41): C, 60.83; H, 4.82; N, 11.82; O, 13.50; S, 9.02. Found: C, 61.11; H, 4.85; N, 11.89.

4.1.4.2. N-(4-Methoxyphenyl)-2-(3-methylbenzofuran-2-carbonyl)-hydrazine-1-carbothioamide (4b**)**. White crystals, mp = 190–193 °C, yield 74%; IR: ν cm⁻¹: 3324, 3228, 3166 (NH groups), 1676 (C=O hydrazide), 1248 (C=S thiosemicarbazide). ¹H NMR (400 MHz, DMSO-d₆) δ 10.63 (s, 1H), 9.75 (s, 1H), 9.68 (s, 1H), 7.81 (d, J = 7.8 Hz, 1H), 7.65 (d, J = 8.3 Hz, 1H), 7.55 (t, J = 7.7 Hz, 1H), 7.40 (t, J = 7.5 Hz, 1H), 7.34 (d, J = 8.1 Hz, 2H), 6.93 (d, J = 8.5 Hz, 2H), 3.78 (s, OCH₃, 3H), 2.61 (s, 3H). ¹³C NMR (100 MHz, DMSO-d₆) 181.71 (C=S), 159.72 (C=O), 157.16, 153.29, 142.61, 132.55, 129.36, 128.69, 127.98, 127.78, 123.77, 122.75, 121.63, 113.64, 112.11, 55.66 (OCH₃), 9.28 (CH₃). Anal. Calcd. for C₁₈H₁₇N₃O₃S (355.41): C, 60.83; H, 4.82; N, 11.82; O, 13.50; S, 9.02. Found: C, 61.07; H, 4.86; N, 11.91.

4.1.4.3. 2-(3-Methylbenzofuran-2-carbonyl)-N-(3-(trifluoromethyl)phenyl)hydrazine-1-carbothioamide (4c**)**. White crystals, mp = 170–172 °C, yield 75%; IR: 3242 (br, NH groups), 1676 (C=O hydrazide), 1256 (C=S thiosemicarbazide). ¹H NMR (400 MHz, DMSO-d₆) δ 10.74 (s, 1H), 10.05 (s, 1H), 10.02 (s, 1H), 7.91 (d, J = 6.9 Hz, 2H), 7.83 (d, J = 7.8 Hz, 1H), 7.67 (d, J = 8.3 Hz, 1H), 7.59 (d, J = 9.3 Hz, 1H), 7.54 (t, J = 7.1 Hz, 2H), 7.41 (t, J = 7.5 Hz, 1H), 2.62 (s, 3H). ¹³C NMR (100 MHz, DMSO-d₆) 181.44 (C=S), 159.76 (C=O), 153.32, 142.42, 140.55, 129.76, 129.33, 128.91, 128.11, 125.92, 123.84, 123.21, 123.21, 122.14, 121.70, 120.51, 112.13, 9.28 (CH₃). Anal.

Calcd. for $C_{18}H_{14}F_3N_3O_2S$ (393.38): C, 54.96; H, 3.59; F, 14.49; N, 10.68; O, 8.13; S, 8.15. Found: C, 55.21; H, 3.61; N, 10.61.

4.1.4.4. *N*-(4-Fluorophenyl)-2-(3-methylbenzofuran-2-carbonyl)hydrazine-1-carbothioamide (4d). White crystals, mp = 206–210 °C, yield 83%; IR: 3305, 3186 (br), (NH groups), 1652 (C=O hydrazide), 1224 (C=S thiosemicarbazide). 1H NMR (400 MHz, DMSO- d_6) δ 10.69 (s, 1H), 9.87 (s, 1H), 9.83 (s, 1H), 7.82 (d, J = 7.7 Hz, 1H), 7.66 (d, J = 8.3 Hz, 1H), 7.58–7.52 (m, 1H), 7.52–7.44 (m, 2H), 7.40 (t, J = 7.3 Hz, 1H), 7.20 (t, J = 8.8 Hz, 2H), 2.61 (s, 3H). Anal. Calcd. for $C_{17}H_{14}FN_3O_2S$ (343.38): C, 59.46; H, 4.11; F, 5.53; N, 12.24; O, 9.32; S, 9.34. Found: C, 59.67; H, 4.08; N, 12.35.

4.1.4.5. *N*-(3-Methoxyphenyl)-2-(3-methylbenzofuran-2-carbonyl)hydrazine-1-carboxamide (6a). White crystals, mp = 162–164 °C, yield 72%; IR: 3354, 3299, 3276 (NH groups), 1711 (C=O hydrazide), 1660 (C=O semicarbazide). 1H NMR (400 MHz, DMSO- d_6) δ 10.37 (s, 1H), 8.90 (s, 1H), 8.25 (s, 1H), 7.81 (d, J = 7.8 Hz, 1H), 7.66 (d, J = 8.3 Hz, 1H), 7.55 (t, J = 7.7 Hz, 1H), 7.41 (t, J = 7.4 Hz, 1H), 7.23–7.13 (m, 2H), 7.06 (d, J = 7.5 Hz, 1H), 6.58 (d, J = 8.0 Hz, 1H), 3.75 (s, OCH₃, 3H), 2.59 (s, 3H). ^{13}C NMR (100 MHz, DMSO- d_6) 160.15 (C=O), 155.77 (C=O of urea), 153.34, 142.48, 141.38, 137.83, 129.89, 129.33, 128.69, 127.97, 125.80, 123.80, 122.69, 121.66, 112.13, 111.3, 55.36 (OCH₃), 9.18 (CH₃). Anal. Calcd. for $C_{18}H_{17}N_3O_4$ (339.35): C, 63.71; H, 5.05; N, 12.38; O, 18.86. Found: C, 63.49; H, 5.09; N, 14.45.

4.1.4.6. *N*-(4-Methoxyphenyl)-2-(3-methylbenzofuran-2-carbonyl)hydrazine-1-carboxamide (6b). White crystals, mp = 236–240 °C, yield 78%; IR: 3370, 3324, 3288 (NH groups), 1681 (C=O hydrazide), 1650 (C=O semicarbazide). 1H NMR (400 MHz, DMSO- d_6) δ 10.34 (s, 1H), 8.72 (s, 1H), 8.16 (s, 1H), 7.81 (d, J = 7.8 Hz, 1H), 7.65 (d, J = 8.3 Hz, 1H), 7.55 (t, J = 7.7 Hz, 1H), 7.48–7.36 (m, 3H), 6.89 (d, J = 8.6 Hz, 2H), 3.74 (s, OCH₃, 3H), 2.59 (s, 3H). ^{13}C NMR (100 MHz, DMSO- d_6) 160.16 (C=O), 156.11 (C=O of urea), 154.94, 153.32, 142.57, 133.18, 129.35, 128.68, 127.92, 125.80, 123.77, 122.56, 121.64, 120.83, 114.27, 112.11, 55.6 (OCH₃), 9.19 (CH₃). Anal. Calcd. for $C_{18}H_{17}N_3O_4$ (339.35): C, 63.71; H, 5.05; N, 12.38; O, 18.86. Found: C, 63.89; H, 5.07; N, 12.46.

4.1.4.7. *N*-(4-Chloro-3-(trifluoromethyl)phenyl)-2-(3-methylbenzofuran-2-carbonyl)hydrazine-1-carboxamide (6c). White crystals, mp = 240–242 °C, yield 80%; IR: 3346, 3296 (br), (NH groups), 1713 (C=O hydrazide), 1662 (C=O semicarbazide). 1H NMR (400 MHz, DMSO- d_6) δ 10.45 (s, 1H), 9.39 (s, 1H), 8.60 (s, 1H), 8.14 (s, 1H), 7.86 (s, 1H), 7.81 (d, J = 7.8 Hz, 1H), 7.65 (t, J = 9.9 Hz, 2H), 7.55 (t, J = 7.7 Hz, 1H), 7.40 (t, J = 7.4 Hz, 1H), 2.60 (s, 3H). ^{13}C NMR (100 MHz, DMSO- d_6) 160.21 (C=O), 155.87 (C=O of urea), 153.35, 142.40, 139.88, 137.82, 132.33, 129.31, 128.67, 127.38, 126.85, 125.78, 124.67, 123.82, 122.91, 119.24, 112.13, 9.18 (CH₃). Anal. Calcd. for $C_{18}H_{13}ClF_3N_3O_3$ (411.77): C, 52.51; H, 3.18; Cl, 8.61; F, 13.84; N, 10.21; O, 11.66. Found: C, 52.37; H, 3.19; N, 10.13.

4.1.4.8. *N*-(3-Methoxyphenyl)-2-(3-(morpholinomethyl)benzofuran-2-carbonyl)hydrazine-1-carbothioamide (15a). White crystals, mp = 190–192 °C, yield 84%; IR: 3262 (br, NH groups), 1647 (C=O hydrazide), 1277 (C=S thiosemicarbazide). 1H NMR (400 MHz, DMSO- d_6) δ 11.95 (s, 1H), 9.86 (s, 2H), 7.99 (d, J = 7.7 Hz, 1H), 7.72 (d, J = 8.2 Hz, 1H), 7.54 (t, J = 7.6 Hz, 1H), 7.42 (t, J = 7.4 Hz, 1H), 7.32–7.17 (m, 2H), 7.10 (d, J = 7.6 Hz, 1H), 6.77 (d, J = 7.8 Hz, 1H), 4.08 (s, 2H), 3.78 (s, OCH₃, 3H), 3.63 (s, 4H, CH₂OCH₂ of morpholinyl moiety), 2.58 (s, 4H, CH₂NCH₂ of morpholinyl moiety). ^{13}C

NMR (100 MHz, DMSO- d_6) 180.98 (C=S), 159.50 (C=O), 153.61, 145.29, 140.77, 137.83, 129.38, 128.74, 128.69, 127.80, 125.80, 124.07, 122.28, 120.90, 118.09, 112.26, 110.82, 66.83 (O(CH₂)₂), 55.56 (OCH₃), 52.95 (N(CH₂)₂), 50.70 (CH₂). Anal. Calcd. for $C_{22}H_{24}N_4O_4S$ (440.52): C, 59.98; H, 5.49; N, 12.72; O, 14.53; S, 7.28. Found: C, 60.24; H, 5.55; N, 12.79.

4.1.4.9. *N*-(4-Methoxyphenyl)-2-(3-(morpholinomethyl)benzofuran-2-carbonyl)hydrazine-1-carbothioamide (15b). White crystals, mp = 198–200 °C, yield 79%; IR: 3273 (br), 3230 (NH groups), 1643 (C=O hydrazide), 1239 (C=S thiosemicarbazide). 1H NMR (400 MHz, DMSO- d_6) δ 11.94 (s, 1H), 9.80 (s, 1H), 9.73 (s, 1H), 7.99 (d, J = 7.8 Hz, 1H), 7.71 (d, J = 8.3 Hz, 1H), 7.54 (t, J = 7.6 Hz, 1H), 7.41 (t, J = 7.4 Hz, 1H), 7.34 (d, J = 6.7 Hz, 2H), 6.94 (d, J = 8.2 Hz, 2H), 4.07 (s, 2H), 3.78 (s, OCH₃, 3H), 3.63 (s, 4H, CH₂OCH₂ of morpholinyl moiety), 2.57 (s, 4H, CH₂NCH₂ of morpholinyl moiety). ^{13}C NMR (100 MHz, DMSO- d_6) 181.60 (C=S), 159.13 (C=O), 157.22, 153.59, 145.29, 132.44, 129.38, 128.76, 128.69, 127.77, 124.04, 122.28, 120.85, 113.81, 112.24, 66.83 (O(CH₂)₂), 55.68 (OCH₃), 52.97 (N(CH₂)₂), 50.74 (CH₂). Anal. Calcd. for $C_{22}H_{24}N_4O_4S$ (440.52): C, 59.98; H, 5.49; N, 12.72; O, 14.53; S, 7.28. Found: C, 60.18; H, 5.47; N, 12.75.

4.1.4.10. 2-(3-(Morpholinomethyl)benzofuran-2-carbonyl)-*N*-(3-(trifluoromethyl)phenyl)hydrazine-1-carbothioamide (15c). White crystals, mp = 210–212 °C, yield 74%; IR: 3449 (br), 3256 (NH groups), 1652 (C=O hydrazide), 1260 (C=S thiosemicarbazide). 1H NMR (400 MHz, DMSO- d_6) δ 11.87 (s, 1H), 10.07 (s, 2H), 8.01 (d, J = 7.8 Hz, 1H), 7.90 (d, J = 7.7 Hz, 2H), 7.72 (d, J = 8.3 Hz, 1H), 7.61 (t, J = 7.8 Hz, 1H), 7.55 (t, J = 7.6 Hz, 2H), 7.42 (t, J = 7.5 Hz, 1H), 4.12 (s, 2H), 3.63 (s, 4H, CH₂OCH₂ of morpholinyl moiety), 2.59 (s, 4H, CH₂NCH₂ of morpholinyl moiety). ^{13}C NMR (100 MHz, DMSO- d_6) 181.10 (C=S), 159.28 (C=O), 153.60, 144.97, 140.57, 129.67, 129.38, 128.71, 127.89, 125.91, 124.09, 123.21, 122.42, 121.89, 120.50, 112.24, 66.44 (O(CH₂)₂), 53.01 (N(CH₂)₂), 50.80 (CH₂). Anal. Calcd. for $C_{22}H_{21}F_3N_4O_3S$ (478.49): C, 55.22; H, 4.42; F, 11.91; N, 11.71; O, 10.03; S, 6.70. Found: C, 55.39; H, 4.38; N, 11.64.

4.1.4.11. *N*-(3-Methoxyphenyl)-2-(3-(morpholinomethyl)benzofuran-2-carbonyl)hydrazine-1-carboxamide (16a). White crystals, mp = 238–240 °C, yield 82%; IR: 3305 (br, NH groups), 1711 (C=O hydrazide), 1640 (C=O semicarbazide). 1H NMR (400 MHz, DMSO- d_6) δ 11.49 (s, 1H), 8.93 (s, 1H), 8.43 (s, 1H), 7.96 (d, J = 7.6 Hz, 1H), 7.67 (d, J = 8.4 Hz, 1H), 7.49 (t, J = 8.0 Hz, 1H), 7.37 (t, J = 7.6 Hz, 1H), 7.16–7.19 (m, 2H), 7.02 (d, J = 7.6 Hz, 1H), 6.57 (d, J = 8.0 Hz, 1H), 4.01 (s, 2H), 3.72 (s, OCH₃, 3H), 3.60 (s, 4H, CH₂OCH₂ of morpholinyl moiety), 2.51 (s, 4H, CH₂NCH₂ of morpholinyl moiety). ^{13}C NMR (100 MHz, DMSO- d_6) 160.07 (C=O), 159.29 (C=O of urea), 155.40, 153.64, 144.99, 141.28, 129.94, 129.38, 128.74, 128.68, 127.75, 124.03, 122.40, 121.03, 112.24, 111.29, 107.78, 104.79, 66.51 (O(CH₂)₂), 55.38 (OCH₃), 53.12 (N(CH₂)₂), 50.89 (CH₂). Anal. Calcd. for $C_{22}H_{24}N_4O_5$ (424.46): C, 62.25; H, 5.70; N, 13.20; O, 18.85. Found: C, 62.47; H, 5.65; N, 13.26.

4.1.4.12. *N*-(4-Methoxyphenyl)-2-(3-(morpholinomethyl)benzofuran-2-carbonyl)hydrazine-1-carboxamide (16b). White crystals, mp = 242–244 °C, yield 73%; IR: 3423, 3320, 3256 (NH groups), 1706 (C=O hydrazide), 1639 (C=O semicarbazide). 1H NMR (400 MHz, DMSO- d_6) δ 11.50 (s, 1H), 8.78 (s, 1H), 8.37 (s, 1H), 8.00 (d, J = 7.8 Hz, 1H), 7.71 (d, J = 8.3 Hz, 1H), 7.54 (t, J = 7.7 Hz, 1H), 7.49–7.26 (m, 4H), 6.90 (d, J = 8.6 Hz, 2H), 4.04 (s, 2H), 3.74 (s, OCH₃, 3H), 3.63 (s, 4H, CH₂OCH₂ of morpholinyl moiety), 2.54 (s,

4H, CH_2NCH_2 of morpholinyl moiety). ^{13}C NMR (100 MHz, $\text{DMSO}-d_6$) 159.31 ($\text{C}=\text{O}$), 155.75 ($\text{C}=\text{O}$ of urea), 155.02, 154.79, 153.63, 145.10, 133.41, 133.05, 128.76, 127.71, 124.02, 122.36, 120.90, 120.85, 120.38, 114.42, 114.33, 112.23, 66.51 ($\text{O}(\text{CH}_2)_2$), 55.61 (OCH_3), 53.11 ($\text{N}(\text{CH}_2)_2$), 50.88 (CH_2). Anal. Calcd. for $\text{C}_{22}\text{H}_{24}\text{N}_4\text{O}_5$ (424.46): C, 62.25; H, 5.70; N, 13.20; O, 18.85. Found: C, 62.01; H, 5.73; N, 13.24.

4.1.5. General method for the synthesis of hydrazones 8a–c, 11, 17a,b and 18

The appropriate hydrazide derivative **2** or **14** (0.6 mmol) was heated at reflux while stirring with suitable aldehyde or ketone derivative (0.7 mmol) in ethanol (8 ml) using catalytic amount of 3–4 drops of glacial acetic acid for 3–7 h. Solvent was then distilled off and the residue was suspended in distilled water while vigorous stirring for 15 min. After filtration and suction drying, the powder obtained was recrystallized from dioxan/isopropyl alcohol mixture to afford the final benzofuran-based hydrazones **8a–c**, **11**, **17a,b** and **18**.

4.1.5.1. N'-(3-Methoxybenzylidene)-3-methylbenzofuran-2-carbohydrazide (8a). White crystals, mp = 242–244 °C, yield 86%; IR: 3222 (NH hydrazone), 2834 (Csp²-H hydrazone) 1653 ($\text{C}=\text{O}$ hydrazone), 1608 ($\text{C}=\text{N}$ hydrazone). ^1H NMR (400 MHz, $\text{DMSO}-d_6$) δ 12.12 (s, 1H), 8.57 (s, 1H), 7.84 (d, J = 7.9 Hz, 1H), 7.69 (d, J = 8.1 Hz, 1H), 7.57 (t, J = 7.3 Hz, 1H), 7.47–7.37 (m, 2H), 7.32 (s, 2H), 7.07 (d, J = 7.4 Hz, 1H), 3.86 (s, OCH_3 , 3H), 2.63 (s, 3H). ^{13}C NMR (100 MHz, $\text{DMSO}-d_6$) 160.04 ($\text{C}=\text{O}$), 156.37 ($\text{C}=\text{O}$ of urea), 153.31, 148.83, 142.52, 136.22, 130.49, 129.48, 128.10, 123.91, 123.41, 121.69, 120.68, 116.85, 112.18, 111.61, 55.67 (OCH_3), 9.29 (CH_3). Anal. Calcd. for $\text{C}_{18}\text{H}_{16}\text{N}_2\text{O}_3$ (308.34): C, 70.12; H, 5.23; N, 9.09; O, 15.57. Found: C, 69.90; H, 5.18; N, 9.13.

4.1.5.2. N'-(4-Methoxybenzylidene)-3-methylbenzofuran-2-carbohydrazide (8b). White crystals, mp = 236–240 °C, yield 83%; IR: 3195 (NH hydrazone), 2836 (Csp²-H hydrazone) 1645 ($\text{C}=\text{O}$ hydrazone), 1606 ($\text{C}=\text{N}$ hydrazone). ^1H NMR (400 MHz, $\text{DMSO}-d_6$) δ 11.97 (s, 1H), 8.54 (s, 1H), 7.81 (d, J = 7.8 Hz, 1H), 7.77–7.63 (m, 3H), 7.55 (t, J = 7.7 Hz, 1H), 7.41 (t, J = 7.5 Hz, 1H), 7.07 (d, J = 8.4 Hz, 2H), 3.85 (s, OCH_3 , 3H), 2.63 (s, 3H). ^{13}C NMR (100 MHz, $\text{DMSO}-d_6$) 161.39 ($\text{C}=\text{O}$), 156.21 ($\text{C}=\text{O}$ of urea), 153.27, 148.85, 142.67, 129.52, 129.26, 127.96, 127.33, 123.84, 123.03, 121.60, 114.84, 112.13, 55.78 (OCH_3), 9.26 (CH_3). Anal. Calcd. for $\text{C}_{18}\text{H}_{16}\text{N}_2\text{O}_3$ (308.34): C, 70.12; H, 5.23; N, 9.09; O, 15.57. Found: C, 69.87; H, 5.20; N, 9.17.

4.1.5.3. N'-(1-(4-Methoxyphenyl)ethylidene)-3-methylbenzofuran-2-carbohydrazide (8c). White crystals, mp = 160 °C, yield 81%; IR: 3393 (NH hydrazone), 1683 ($\text{C}=\text{O}$ hydrazone), 1607 ($\text{C}=\text{N}$ hydrazone). ^1H NMR (400 MHz, $\text{DMSO}-d_6$) δ 10.70 (s, 1H), 7.87 (d, J = 8.0 Hz, 2H), 7.81 (d, J = 7.8 Hz, 1H), 7.70 (d, J = 8.3 Hz, 1H), 7.55 (t, J = 7.7 Hz, 1H), 7.40 (t, J = 7.5 Hz, 1H), 7.04 (d, J = 8.4 Hz, 2H), 3.84 (s, OCH_3 , 3H), 2.61 (s, 3H), 2.40 (s, 3H). ^{13}C NMR (100 MHz, $\text{DMSO}-d_6$) 161.03 ($\text{C}=\text{O}$), 156.64 ($\text{C}=\text{O}$ of urea), 153.35, 143.04, 130.66, 129.47, 129.09, 128.53, 127.83, 123.81, 122.45, 121.55, 114.22, 112.24, 55.72 (OCH_3), 14.75 (CH_3 of acetophenone), 9.27 (CH_3). Anal. Calcd. for $\text{C}_{19}\text{H}_{18}\text{N}_2\text{O}_3$ (322.36): C, 70.79; H, 5.63; N, 8.69; O, 14.89. Found: C, 70.96; H, 5.67; N, 8.60.

4.1.5.4. N'-(3,4-Dihydronaphthalen-1(2H)-ylidene)-3-methylbenzofuran-2-carbohydrazide (11). White crystals, mp = 180–182 °C, yield 89%; IR: 3383 (NH hydrazone), 1686 ($\text{C}=\text{O}$ hydrazone), 1607

($\text{C}=\text{N}$ hydrazone). ^1H NMR (400 MHz, $\text{DMSO}-d_6$) δ 10.67 (s, 1H), 8.14 (d, 1H), 7.82 (d, J = 7.8 Hz, 1H), 7.71 (d, J = 8.3 Hz, 1H), 7.55 (t, J = 7.7 Hz, 1H), 7.41 (t, 1H), 7.36 (d, J = 7.2 Hz, 1H), 7.32 (d, J = 7.3 Hz, 1H), 7.27 (d, J = 7.4 Hz, 1H), 2.85 (dt, J = 12.0, 5.9 Hz, 4H), 2.62 (s, 3H), 1.91 (p, J = 6.3 Hz, 2H). ^{13}C NMR (100 MHz, $\text{DMSO}-d_6$) 156.56 ($\text{C}=\text{O}$), 155.98, 153.37, 143.01, 140.79, 132.55, 130.10, 129.46, 129.15, 127.89, 126.76, 125.23, 123.83, 122.60, 121.59, 112.25, 29.35 (CH_2 of C-4 of dihydronaphthalen-1(2H)-one), 26.42 (CH_2 of C-3 of dihydronaphthalen-1(2H)-one), 21.88 (CH_2 of C-2 of dihydronaphthalen-1(2H)-one), 9.29 (CH_3). Anal. Calcd. for $\text{C}_{20}\text{H}_{18}\text{N}_2\text{O}_2$ (318.38): C, 75.45; H, 5.70; N, 8.80; O, 10.05. Found: C, 75.21; H, 5.71; N, 8.83.

4.1.5.5. N'-(Benzylidene-3-(morpholinomethyl)benzofuran-2-carbohydrazide (17a). White crystals, mp = 174 °C, yield 85%; ^1H NMR (400 MHz, $\text{DMSO}-d_6$) δ 12.72 (s, 1H), 8.52 (s, 1H), 8.02 (d, J = 7.8 Hz, 1H), 7.79 (d, J = 6.6 Hz, 2H), 7.72 (d, J = 8.3 Hz, 1H), 7.59–7.46 (m, 4H), 7.42 (t, J = 7.5 Hz, 1H), 4.09 (s, 2H), 3.64 (s, 4H, CH_2OCH_2 of morpholinyl moiety), 3.54 (s, 4H, CH_2NCH_2 of morpholinyl moiety). ^{13}C NMR (100 MHz, $\text{DMSO}-d_6$) 156.00 ($\text{C}=\text{O}$), 153.65, 149.06, 144.84, 134.61, 130.81, 129.37, 128.89, 127.90, 127.73, 124.09, 122.64, 121.79, 112.26, 66.62 ($\text{O}(\text{CH}_2)_2$), 53.30 ($\text{N}(\text{CH}_2)_2$), 51.07 (CH_2). Anal. Calcd. for $\text{C}_{21}\text{H}_{21}\text{N}_3\text{O}_3$ (363.42): C, 69.41; H, 5.82; N, 11.56; O, 13.21. Found: C, 69.60; H, 5.89; N, 11.62.

4.1.5.6. N'-(4-Methoxybenzylidene)-3-(morpholinomethyl)benzofuran-2-carbohydrazide (17b). White crystals, mp = 200 °C, yield 79%; IR: 3449 (br, NH hydrazone), 2844 (Csp²-H hydrazone) 1681 ($\text{C}=\text{O}$ hydrazone), 1611 ($\text{C}=\text{N}$ hydrazone). ^1H NMR (400 MHz, $\text{DMSO}-d_6$) δ 12.60 (s, 1H), 8.44 (s, 1H), 8.01 (d, J = 7.8 Hz, 1H), 7.73 (d, J = 7.4 Hz, 2H), 7.71 (s, 1H), 7.54 (t, J = 7.7 Hz, 1H), 7.41 (t, J = 7.4 Hz, 1H), 7.08 (d, J = 8.2 Hz, 2H), 4.08 (s, 2H), 3.85 (s, OCH_3 , 3H), 3.64 (s, 4H, CH_2OCH_2 of morpholinyl moiety), 2.54 (s, 4H, CH_2NCH_2 of morpholinyl moiety). ^{13}C NMR (100 MHz, $\text{DMSO}-d_6$) 161.50 ($\text{C}=\text{O}$), 155.82, 153.61, 148.92, 145.01, 129.38, 128.92, 127.79, 127.14, 124.06, 122.56, 121.42, 114.86, 112.24, 66.61 ($\text{O}(\text{CH}_2)_2$), 55.81 (OCH_3), 53.28 ($\text{N}(\text{CH}_2)_2$), 51.05 (CH_2). Anal. Calcd. for $\text{C}_{22}\text{H}_{23}\text{N}_3\text{O}_4$ (393.44): C, 67.16; H, 5.89; N, 10.68; O, 16.27. Found: C, 67.03; H, 5.91; N, 16.36.

4.1.5.7. N'-(3,4-Dihydronaphthalen-1(2H)-ylidene)-3-(morpholinomethyl)benzofuran-2-carbohydrazide (18). White crystals, mp = 200 °C, yield 87%; IR: 3449 (br, NH hydrazone), 1685 ($\text{C}=\text{O}$ hydrazone), 1618 ($\text{C}=\text{N}$ hydrazone). ^1H NMR (400 MHz, $\text{DMSO}-d_6$) δ 11.31 (s, 1H), 8.16 (d, J = 7.4 Hz, 1H), 8.02 (d, J = 7.8 Hz, 1H), 7.75 (d, J = 8.2 Hz, 1H), 7.55 (t, J = 7.7 Hz, 1H), 7.42 (t, J = 7.5 Hz, 1H), 7.40–7.30 (m, 2H), 7.27 (d, J = 7.3 Hz, 1H), 4.04 (s, 2H), 3.64 (s, 4H, CH_2OCH_2 of morpholinyl moiety), 2.52 (s, 4H, CH_2NCH_2 of morpholinyl moiety), 2.84 (s, 4H), 2.06–1.83 (m, 2H). ^{13}C NMR (100 MHz, $\text{DMSO}-d_6$) 155.97 ($\text{C}=\text{O}$), 154.56, 153.77, 145.67, 140.78, 132.47, 130.10, 129.15, 129.07, 127.78, 126.79, 125.25, 124.10, 122.26, 120.04, 112.34, 66.23 ($\text{O}(\text{CH}_2)_2$), 53.51 ($\text{N}(\text{CH}_2)_2$), 50.94 (CH_2), 29.26 (CH_2 of C-4 of dihydronaphthalen-1(2H)-one), 26.91 (CH_2 of C-3 of dihydronaphthalen-1(2H)-one), 21.75 (CH_2 of C-2 of dihydronaphthalen-1(2H)-one). Anal. Calcd. for $\text{C}_{24}\text{H}_{25}\text{N}_3\text{O}_3$ (403.48): C, 71.44; H, 6.25; N, 10.41; O, 11.90. Found: C, 71.63; H, 6.28; N, 10.43.

4.2. Biological evaluation

The procedures of experiments performed for the biological evaluations in this study have been provided in the Supporting materials.

4.3. In silico ADME calculation

Vina Autodock software, freely available online, was used to conduct the docking studies as it achieves more accuracy and twice speed higher than Autodock 4 software³⁹. The crystal structure of the VEGFR in complex with Sorafenib was obtained from the protein data bank PDB ID (4ASD)³⁷. As Vina Autodock requires both the receptor and the ligands in pdbqt format plus the coordinates and the size of a grid box surrounding the binding site. For that, M.G.L tools were used to prepare the needed files in the right format besides, generating a grid box surrounding the binding site of Sorafenib with VEGFR protein⁴⁰. Rough validation of the docking protocol has been achieved through re-docking the co-crystallized ligand to its corresponding enzyme once in water presence and another time in water absence and then the RMSD was calculated. Finally, the three synthesised lead compounds were docked into VEGFR enzyme. The docking results were visualised by Biovia discovery studio 2020 free visualiser (<https://3dsbiovia.com/resource-center/downloads/>) that was used to generate 2D and 3D interactions for the docked compounds.

Acknowledgements

The authors extend their sincere appreciation to the central laboratory at Jouf University for support this study. M. M. Al-Sanea also extends his appreciation to the Korea Institute of Science and Technology (KIST) for funding this work through the Grant name "2021 KIST School Partnership Project."

Disclosure statement

No potential conflict of interest was reported by the author(s).

Funding

The authors extend their appreciation to the Deputyship for Research & Innovation, Ministry of Education in Saudi Arabia for funding this work through the project number "375213500."

References

- Bray F, Ferlay J, Soerjomataram I, et al. Global cancer statistics 2018: GLOBOCAN estimates of incidence and mortality worldwide for 36 cancers in 185 countries. *CA Cancer J Clin* 2018;68:394–424.
- Alonso R, Pineros M, Lavrsanne M, et al. Lung cancer incidence trends in Uruguay 1990–2014: an age-period-cohort analysis. *Cancer Epidemiol* 2018;55:17–22.
- Lortet-Tieulent J, Renteria E, Sharp L, et al. Convergence of decreasing male and increasing female incidence rates in major tobacco-related cancers in Europe in 1988–2010. *Eur J Cancer* 2015;51:1144–63.
- Bistrovic A, Krstulovic L, Harej A, et al. Design, synthesis and biological evaluation of novel benzimidazole amidines as potent multi-target inhibitors for the treatment of non-small cell lung cancer. *Eur J Med Chem* 2017;143:1616.
- Almahli H, Hadchity E, Jaballah MY, et al. Development of novel synthesised phthalazinone-based PARP-1 inhibitors with apoptosis inducing mechanism in lung cancer. *Bioorg Chem* 2018;77:443–56.
- Atal S, Asokan P, Jhaj R. Recent advances in targeted small-molecule inhibitor therapy for non-small-cell lung cancer—an update. *J Clin Pharm Ther* 2020;45:580–4.
- Nevagi RJ, Dighe SN, Dighe SN. Biological and medicinal significance of benzofuran. *Eur J Med Chem* 2015;97:561–81.
- Miao Y-h, Hu Y-h, Yang J, et al. Natural source, bioactivity and synthesis of benzofuran derivatives. *RSC Adv* 2019;9:27510–40.
- Radadiya A, Shah A. Bioactive benzofuran derivatives: an insight on lead developments, radioligands and advances of the last decade. *Eur J Med Chem* 2015;97:356–76.
- Shamsuzzaman HK. Bioactive Benzofuran derivatives: a review. *Eur J Med Chem* 2015;97:483–504.95.
- Abdelrahman MA, Eldehna WM, Nocentini A, et al. Novel benzofuran-based sulphonamides as selective carbonic anhydrases IX and XII inhibitors: synthesis and in vitro biological evaluation. *J Enzyme Inhib Med Chem* 2020;35:298–305.
- Shaldam M, Eldehna WM, Nocentini A, et al. Development of novel benzofuran-based SLC-0111 analogs as selective cancer-associated carbonic anhydrase isoform IX inhibitors. *Eur J Med Chem* 2021;216:113283.
- Chand K, Rajeshwari, Hiremathad A, et al. A review on anti-oxidant potential of bioactive heterocycle benzofuran: natural and synthetic derivatives. *Pharmacol Rep* 2017;69:281–95.
- Goyal D, Kaur A, Goyal B. Benzofuran and indole: promising scaffolds for drug development in Alzheimer's disease. *ChemMedChem* 2018;13:1275–99.
- Alizadeh M, Jalal M, Hamed K, et al. Recent updates on anti-inflammatory and antimicrobial effects of furan natural derivatives. *J Inflamm Res* 2020;13:451–63.
- Hiremathad A, Patil MR, Chand K, et al. Benzofuran: an emerging scaffold for antimicrobial agents. *RSC Adv* 2015;5:96809.
- Xu Z, Zhao S, Zaosheng L, et al. Benzofuran derivatives and their anti-tubercular, anti-bacterial activities. *Eur J Med Chem* 2019;162:266–76.
- Kwiecień H, Goszczyńska A, Rokosz P. Benzofuran small molecules as potential inhibitors of human protein kinases. A review. *Curr Pharm Des* 2016;22:879–94.
- Eldehna WM, Al-Rashood ST, Al-Warhi T, et al. Novel oxindole/benzofuran hybrids as potential dual CDK2/GSK-3 β inhibitors targeting breast cancer: design, synthesis, biological evaluation, and in silico studies. *J Enzyme Inhib Med Chem* 2021;36:270–85.
- Gao C, Sun X, Wu Z, et al. A novel benzofuran derivative Moracin N induces autophagy and apoptosis through ROS generation in lung cancer. *Front Pharmacol* 2020;11:391.
- Abbas HS, Abd El-Karim SS. Design, synthesis and anticervical cancer activity of new benzofuran-pyrazol-hydrazonothiazolidin-4-one hybrids as potential EGFR inhibitors and apoptosis inducing agents. *Bioorg Chem* 2019;89:103035.
- Mphahlele MJ, Maluleka MM, Aro A, et al. Benzofuran-appended 4-aminoquinazoline hybrids as epidermal growth factor receptor tyrosine kinase inhibitors: synthesis, biological evaluation and molecular docking studies. *J Enzyme Inhib Med Chem* 2018;33:1516–28.
- Eldehna WM, Nocentini A, Elsayed ZM, et al. Benzofuran-based carboxylic acids as carbonic anhydrase inhibitors and antiproliferative agents against breast cancer. *ACS Med Chem Lett* 2020;11:1022–7.

24. Zou Y. Benzofuran-isatin conjugates as potent VEGFR-2 and cancer cell growth inhibitors. *J Heterocycl Chem* 2020;57: 510–6.
25. Abdelhafez OM, Amin KM, Ali HI, et al. Design, synthesis and anticancer activity of benzofuran derivatives targeting VEGFR-2 tyrosine kinase. *RSC Adv* 2014;4:11569–79.
26. Abdelhafez OM, Ali HI, Amin KM, Abdalla MM. Design, synthesis and anticancer activity of furochromone and benzofuran derivatives targeting VEGFR-2 tyrosine kinase. *RSC Adv* 2015;5:25312–24.
27. Modi SJ, Kulkarni VM. Vascular endothelial growth factor receptor (VEGFR-2)/KDR inhibitors: medicinal chemistry perspective. *Med Drug Discov* 2019;2:100009.
28. Eldehna WM, El Kerdawy AM, Al-Ansary GH, et al. Type IIA–Type IIB protein tyrosine kinase inhibitors hybridization as an efficient approach for potent multikinase inhibitor development: design, synthesis, anti-proliferative activity, multikinase inhibitory activity and molecular modeling of novel indolinone-based ureides and amides. *Eur J Med Chem* 2019;163:37–53.
29. Sun Q, Zhou J, Zhang Z, et al. Discovery of fruquintinib, a potent and highly selective small molecule inhibitor of VEGFR 1, 2, 3 tyrosine kinases for cancer therapy. *Cancer Biol Ther* 2014;15:1635–45.
30. Shirley M. Fruquintinib: first global approval. *Drugs* 2018;78: 1757–61.
31. Lu S, Chen G, Sun Y, et al. A Phase III, randomized, double-blind, placebo-controlled, multicenter study of fruquintinib in Chinese patients with advanced nonsquamous non-small-cell lung cancer–The FALUCA study. *Lung Cancer* 2020;146: 252–62.
32. Bruce JY, LoRusso PM, Goncalves PH, et al. A pharmacodynamically guided dose selection of PF-00337210 in a phase I study in patients with advanced solid tumors. *Cancer Chemother Pharmacol* 2016;77:527–38.
33. Ho T-L. Hard soft acids bases (HSAB) principle and organic chemistry. *Chem Rev* 1975;75:1–20.
34. Mosmann T. Rapid colorimetric assay for cellular growth and survival: application to proliferation and cytotoxicity assays. *J Immunol Methods* 1983;65:55–63.
35. Engels EA. Inflammation in the development of lung cancer: epidemiological evidence. *Expert Rev Anticancer Ther* 2008; 8:605–15.
36. Franzblau SG, Witzig RS, McLaughlin JC, et al. Rapid, low-technology MIC determination with clinical *Mycobacterium tuberculosis* isolates by using the microplate Alamar Blue assay. *J Clin Microbiol* 1998;36:362–6.
37. McTigue M, Murray BW, Chen JH, et al. Molecular conformations, interactions, and properties associated with drug efficiency and clinical performance among VEGFR TK inhibitors. *Proc Natl Acad Sci* 2012;109:18281–9.
38. Grubenmann W, Erlenmeyer H. Über bromierte Cumaronderivate und über eine neue Darstellung von Cumaronyl-3-essigsäure. *Helv Chim Acta* 1948;31: 78–83.
39. Trott O, Olson AJ. AutoDock Vina: improving the speed and accuracy of docking with a new scoring function, efficient optimization and multithreading. *J Comput Chem* 2010;31:455–61.
40. Morris GM, Huey R, Lindstrom W, et al. Autodock4 and AutoDockTools4: automated docking with selective receptor flexibility. *J Comput Chem* 2009;30:2785–91.